1 **Functionally conserved non-coding regulators of cardiomyocyte proliferation and regeneration**

2 **in mouse and human.**

3 Adamowicz, Morgan, Haubner

4 Transcriptomic regulation of cardiac regeneration.

5 Martyna Adamowicz[2,9], Claire C. Morgan[2,5,9], Bernhard J. Haubner[3,4,9], Michela Noseda[2], Melissa J.

6 Collins[5], Marta Abreu Paiva[2], Prashant K. Srivastava[5], Pascal Gellert[6], Bonnie Razzaghi[5], Peter

7 O'Gara[2], Priyanka Raina[5], Laurence Game[7], Leonardo Bottolo[8], Michael D. Schneider[2], Sian E.

8 Harding[2], Josef Penninger[3,10] and Timothy J. Aitman[1,5,10,11]

9 [1]Centre for Genomic and Experimental Medicine, Institute of Genetics and Molecular Medicine,

10 University of Edinburgh, Edinburgh, UK

11 [2]National Heart and Lung Institute, Faculty of Medicine, Imperial College, London, UK

12 [3]IMBA, Institute of Molecular Biotechnology of the Austrian Academy of Sciences, Vienna, Austria

13 [4]Department of Internal Medicine III, Medical University of Innsbruck, Austria

14 [5]Department of Medicine, Faculty of Medicine, Imperial College, London, UK

15 [6]Physiological Genomics and Medicine, MRC Clinical Sciences Centre, London, UK

16 [7]Genomics Core Laboratory, MRC Clinical Sciences Centre, London, UK

17 [8]Department of Mathematics, Faculty of Natural Sciences, Imperial College, London, UK

18 [9]co-first authors

19 [10]co-senior authors

20 [11]To whom correspondence should be addressed: tim.aitman@ed.ac.uk

21 Word count: 6978

22   **Abstract**

23   **Rationale**

24   The adult mammalian heart has little regenerative capacity after myocardial infarction (MI) while

25   neonatal mouse heart regenerates without scarring or dysfunction. However, the underlying pathways

26   are poorly defined.

27   **Objective**

28   We sought to derive insights into the pathways regulating neonatal development of the mouse heart and

29   cardiac regeneration post-MI.

30   **Methods and Results**

31   Total RNA-seq of normal mouse heart through the first 10 days of postnatal life revealed a previously

32   unobserved transition in microRNA expression between P3 and P5 that associates specifically with

33   altered expression of protein-coding genes on the focal adhesion pathway and cessation of

34   cardiomyocyte cell division. We also found profound changes in the coding and non-coding

35   transcriptome after neonatal MI, with evidence of essentially complete healing by P10. Over two thirds

36   of each of the mRNAs, lncRNAs and microRNAs that were differentially expressed in the post-MI

37   heart were also differentially expressed during normal postnatal development, suggesting a common

38   regulatory pathway for normal cardiac development and post-MI cardiac regeneration. We selected

39   exemplars of miRNAs that were implicated in our data set as regulators of cardiomyocyte proliferation.

40   Several of these showed evidence of a functional influence on mouse cardiomyocyte cell division. In

41   addition, a subset of these microRNAs, miR-144-3p, miR-195a-5p, miR-451a and miR-6240 showed

42   evidence of functional conservation in human cardiomyocytes.

43   **Conclusions**

44　The sets of mRNAs, miRNAs and lncRNAs that we report here merit further investigation as

45　gatekeepers of cell division in the postnatal heart and as targets for extension of the period of cardiac

46　regeneration beyond the neonatal period.

47

Background

Heart disease is amongst the commonest causes of death worldwide [1]. Whilst planarians, teleost fish and some amphibians have the ability to regrow limbs or organs including the heart [2-4], mammals are limited in their regenerative abilities [5, 6]. Following myocardial infarction (MI), damaged myocardium is replaced by scar tissue triggering cardiac remodelling and impaired cardiac function [7, 8].

A major barrier to cardiac regeneration in adult mammals is the withdrawal of the cardiomyocyte from the cell cycle in early postnatal life. In the mouse, although DNA replication continues in the first week of postnatal life, cytokinesis ceases. By the second week of life, mouse cardiomyocytes withdraw from the cell cycle, 90% of cardiomyocytes are binucleated and, aside from a recent report of a proliferative burst at P15 [9], recently contested [10], heart growth after the first week of life occurs mainly through cardiomyocyte hypertrophy rather than proliferation [11, 12]. This programme of cell cycle arrest is hypothesised to result from metabolic, physiological and anatomical changes in the first week of life including a shift to oxidative metabolism with relative hyperoxia compared to foetal life, increasing ventricular pressure and accumulation of extracellular matrix [13]. These considerations raised the possibility that regeneration of the mouse heart could follow cardiac injury in the immediate neonatal period and indeed complete cardiac regeneration has recently been demonstrated following apex resection and infarction of the mouse left ventricle (LV) on the first day of postnatal life [14-16].

Transcriptome analyses in planarians and amphibians have yielded significant insights into the regulatory mechanisms underlying tissue and organ regeneration in these species [17-19] but morphological, physiological and genetic differences between these species and mammals limit the translational potential for application to human disease. They do, however provide the basis of the molecular investigations in mammals [19]. In mice, the role of individual microRNAs (miRNAs) and protein-coding messenger RNAs (mRNAs) have been defined by genetic analyses and gene targeting of specified mRNAs and miRNAs [16, 20, 21]. More recently with recognition of the functions of other RNA species, certain long non-coding RNAs (lncRNAs) have been implicated in cardiac biology [22], for example, in protection from cardiac hypertrophy, foetal heart development, and autophagic cell

75   death in myocardial infarction [23-26]. Although previous genome-wide studies have examined the

76   coding transcriptome in neonatal and regenerating heart following apical resection [27], genome-wide

77   changes in the non-coding transcriptome have not been reported.

78   Here we have performed an in-depth analysis of the coding and non-coding mouse LV transcriptome

79   by RNA sequencing at key time points in early postnatal mouse heart development and in the LV during

80   the period of regeneration following neonatal ligation of the left anterior descending coronary artery

81   (LAD). The study defines the major sets of coding and non-coding RNAs associated with normal

82   postnatal cardiac development and with regeneration of the neonatal heart following MI. We perform

83   functional studies on a key set of exemplar miRNAs in mouse and human cardiomyocytes and identify

84   conserved roles for these miRNAs in mammalian cardiomyocyte proliferation and mitosis. Our study

85   provides new insights into the transcriptional regulation of neonatal cardiac development and

86   regeneration in mammals that will be of value in future comparative and human intervention studies of

87   cardiac regeneration.

88   **Materials and Methods**

89   Left anterior descending artery (LAD) ligation was performed in P0.5 neonatal C57BL6J mice, as

90   previously described [15]. Left ventricle (LV) was harvested from three C57BL6J mice from sham-

91   operated and LAD-ligated animals at three, five, seven and 10-days post ligation. Left ventricle (LV)

92   was also harvested from three C57BL6J mice at P1, P3, P5, P7, P10 (referred to as physiological time

93   points) in which no surgical procedures had been performed. Coding and non-coding RNA-Seq libraries

94   were prepared using Illumina TruSeq stranded RNA library preparation and TruSeq small RNA library

95   preparation kits following manufacturers' protocols. Mouse genome assembly GCRm38/mm10 and the

96   Ensembl transcript annotations (version GRCm38.87) were used as the reference sequence in all the

97   analyses. RNA-Seq reads were quantified using Salmon (v.0.8.2) [28]. Differential expression (DE)

98   analysis was performed using DESeq2 Bioconductor package. Raw p values were adjusted for multiple

99   testing with the Benjamini-Hochberg procedure. Weighted gene co-expression cluster analysis

100   (WGCNA) and a short timer series expression miner (STEM) analysis were performed to identify

101 clusters of co-expressed mRNAs. Enrichment of KEGG Pathways for DE mRNAs was calculated using

102 DAVID (v6.8) across all pairwise comparisons. MiRNA-Seq reads were aligned with Bowtie and

103 MirDeep2 was used to determine the presence and quantity of miRNAs based on mouse precursor

104 sequences and mature sequences from mouse and rat with miRBase release 19. MiRNA binding sites

105 were predicted in-silico across each gene using the union of five separate prediction methods.

106 Correlation matrices were generated between mRNAs and miRNAs and between mRNAs and

107 lncRNAs. Potential functional relationships were identified by Spearman correlation, adjusted for

108 multiple testing correction at FDR < 0.05. P5 mouse cardiomyocytes were treated with mmu-miR-22-

109 5p, mmu-miR-144, mmu-miR-148a-3p, mmu-miR-193a-3p, mmu-miR-193b-3p, mmu-miR-221-3p,

110 mmu-miR-331-3p, mmu-miR-451a inhibitors and mmu-miR-6240 mimic and iCell® Cardiomyocytes

111 were treated with human analogues of these miRs. Cells were incubated 10 μM EdU 4 h after seeding

112 and subsequently fixed with 4% paraformaldehyde and permeabilized in 0.2% (v/v) Triton X-100

113 before incubation with Click-iT reaction. Hoechst was used for nuclear staining and pH3 to mark mitotic

114 cells. The analysis was then performed with conventional epifluorescence microscopy.

115 **Results**

116 To define the transcriptional changes occurring during physiological postnatal cardiac development and

117 after neonatal MI, we generated RNA-Seq expression data of the coding and non-coding transcriptome

118 from triplicate LV tissue harvested from C57BL/6 mice on postnatal day 0.5, 3.5, 5.5, 7.5 and 10.5,

119 referred to as P1, P3, P5, P7 and P10, and from LV at 3 to 10 days following LAD ligation (Figure 1).

120 **Transcriptional changes in coding RNA**

121 During the time course of physiological postnatal growth from P1 to P10, we identified 9,450 unique

122 differentially expressed (DE) mRNAs across all possible pairwise comparisons (Data supplement 1).

123 We identified an increase in gene expression of 11 cardiomyocyte markers at different time points and

124 an increase in cardiac fibroblast marker (*Ddr2*) after P5, reflecting the change in cellular composition

125 within the LV (Data supplement 2A). WGCNA and STEM analyses of these genes identified clusters

126 enriched for focal adhesion (p-adj = 1.22E-13), DNA replication (5.47E-16), ribosome (1.64E-50) and

127   OXPHOS (p-adj = 0.013) pathways of KEGG analysis (Data supplement 3A, B). These results were

128   affirmed in pairwise comparisons between time points, with enrichment for DNA replication genes

129   between P1 and P5, oxidative phosphorylation, focal adhesion genes between P3 and P10, and

130   ribosomal transcripts throughout a 10-day period (Figure 2A, Data supplement 4). Investigation of

131   pairwise comparisons between adjacent time points revealed a sharp increase in the number of

132   differentially expressed genes (DEG) from between P3 to P5 (494) to P5 to P7 (3,545), with the largest

133   number identified between P7 and P10 (4,375) (Figure 2B Data supplement 5A). Of the 40 most DEG

134   between P5 and P7, 10 genes (*Ube2c, Kif20a, Top2a, Racgap1, Cdca3, Cenpf, Ccna2, Iqgap3, Anln,*

135   *Ccnb1 and CenpE)* had GO terms associated with mitotic cell cycle process all of which were

136   downregulated between P5 and P7 (Figure 2C, Data supplement 3).

137   Following sham operation and LAD ligation, transcriptome analysis showed a large number of DEG

138   between sham-operated and LAD-ligated mice three days after injury (ShamvLAD (P3) = 2,741). The

139   number of DEG declined very sharply three days post ligation, with 499 genes found to be DE between

140   sham and LAD at P5, 112 between sham and LAD at P7, and 61 between sham and LAD-ligated at P10

141   (Figure 2D, Data supplement 5B). Upregulation of sarcomere expressed *Mypn* and cardiac fibroblast

142   marker *Ddr2* was observed following LAD ligation at P3 with restoration of physiological expression

143   profile of cardiomyocyte markers from P7 (Data supplement 2B).

144   STEM analysis of the post-LAD ligation data showed 15 statistically significant profiles of changing

145   gene expression, which had generally decreasing gene expression related to immune processes such as

146   phagosome (p-adj = 5.9E-9) and cytokine-cytokine receptor interaction (p-adj=8.77E-8) (Data

147   supplement 3C). Four profiles (40, 42, 48 and 49) showed increasing gene expression pattern and were

148   significantly enriched for OXPHOS which was also observed in the WGCNA analysis (Data

149   supplement 3C, D). STEM analysis of mRNA expression in the sham-operated mice (P3-P10) showed

150   pathway enrichment for 13 profiles, mirroring enrichments observed in the physiological samples.

151   Consistent with the STEM annotation analysis, pairwise comparisons of the sham and LAD data at P3

152   showed that the major classes of DEG between P3 sham and LAD were within OXPHOS and lysosome

153 pathways (Figure 2E, Data supplement 4). Of the top 40 most significant DE mRNAs, we identified

154 five genes (*Fn1*, *Col1a1*, *Tnc*, *Thbs1* and *Col1a2*) with an increase in expression between sham and

155 LAD at P3 that are implicated in focal adhesion pathways and three genes (*Cd68*, *Laptm5* and

156 *Atp6v0d2*) representing lysosome pathways (Figure 2E, F). Strikingly, 74% of the 3,210 genes that were

157 DE between sham and LAD were also DE in the pairwise comparisons in the normal physiological data

158 (Figure 2G). Of the 10,284 DEG, 20 were validated and further characterised by qPCR across all

159 conditions used in the study using an independent set of triplicate samples (Data supplement 6A).

160 **Changes in non-coding RNA transcriptome**

161 Next, we analysed changes in the expression of non-coding RNAs including lncRNAs and miRNAs in

162 the normal developing heart. Between all pairwise time point comparisons from P1 to P10, we identified

163 545 unique DE lncRNAs (Data supplement 1). A fourfold increase in the number of DE lncRNAs was

164 observed between P3 and P5 (n=24) and between P5 and P7 (n=107) comparisons (Figure 3A). Only

165 59 of 545 DE lncRNAs have assigned names, for the remainder, there has been limited, functional

166 characterisation. Four DE lncRNAs between P5vP7, within the top 40 DE, that have names and

167 functions associated with them include: *Nespas, Sorbs2os, H19 and Lockd* (Figure 3B, Supplementary

168 dataset 1). This is the first report showing DE of any of these lncRNAs in the postnatal mammalian

169 heart.

170 To explore potential interactions between lncRNAs and mRNAs in the developing heart, we tested for

171 correlation between lncRNA and mRNA expression across P1 to P10 time points. Of the 545 DE

172 lncRNAs, 491 correlated significantly (p-adj$_{Spearman}$ < 0.05) with between 1 and 2,604 mRNAs either in

173 *cis* or *trans*. Overall, we found that there were slightly more (median = 26) lncRNAs significantly

174 correlating in *trans* compared to in *cis* (median = 15), implying that their regulatory potential is not

175 limited by chromosomal location (Figure 3C).

176 To determine possible functional regulatory roles of DE lncRNAs, we performed a KEGG analysis on

177 the sets of genes correlating in *cis* or *trans* with DE lncRNAs. We identified 86 lncRNAs that correlated

178 significantly with gene sets enriched for the ribosome pathway, 113 for oxidative phosphorylation, and

179 103 with enrichment for the focal adhesion pathway (Data supplement 7).

180 Between sham-operated and LAD-ligated LV at P3 we identified 51 DE lncRNAs, 55 DE lncRNA at

181 P5 and eight DE lncRNAs at P7. No DE lncRNAs were identified at P10 (Figure 3E, Data supplement

182 1), in keeping with the marked reduction in DE mRNAs and miRNAs at later time points. The 51 DE

183 lncRNAs between sham and LAD comparisons at P3 include the known lncRNAs *H19*, *Dnm3os*, *Lockd*,

184 *Malat1*, *Meg3*, *Mhrt*, *Mirt1*, *Neat1*, *Slmapos2*, *Zfp469* and 41 lncRNAs with unknown function (Figure

185 3E). A selection of these lncRNAs was significantly correlated with gene sets enriched in ribosome,

186 OXPHOS, focal adhesion, lysosome and phagosome KEGG pathways (Data supplement 7). Seventy

187 three of the 109 DE lncRNAs (67%) between sham and LAD were also DE between time points in the

188 physiological samples (Figure 3F, Data supplement 7).

189 Analysis of small RNAs identified 413 DE miRNAs across all pairwise comparisons of physiological

190 time points (Data supplement 8). Expression of 22 of 413 DE miRNAs was tested in separate samples

191 from different animals, in all time points by qPCR and these were all validated (Data supplement 6B).

192 The changes were also validated in sorted cells' subpopulations, showing that the change of expression

193 occurred both in cardiomyocytes and endothelial cells (data not shown). Of the 413 DE miRNAs, 240

194 were DE between the P3vP5 time points, 197 were unique (Figure 4A, Data supplement 8). The marked

195 transition in expression of these miRNAs, between P3 and P5, has not previously been observed.

196 To identify the potential roles of DE miRNAs during the P1 to P10 time period, we examined the

197 correlation between the 413 miRNAs that were DE between all the time points and all mRNAs

198 expressed in these samples, and intersected these data with the *in silico* predicted binding partners of

199 the DE miRNAs to give a set of RNAs that correlate with and may be targeted by these miRNAs (Data

200 supplement 9). We identified 65 unique miRNAs where their significantly correlated gene targets are

201 enriched for specific KEGG pathways, 34 of which target a total of 67 genes associated with the focal

202 adhesion pathway (Data supplement 10). Interestingly, orthologues of 49 of these 65 miRNAs were

203 also identified in the human genome and these showed conservation of gene targets for a median of

204 84% of the orthologous genes within the human pathways (Data supplement 10).

205 We also investigated the temporal relationship between miRNAs and mRNAs. The 240 DE miRNAs,

206 identified between P3 and P5, are predicted to target 2,731 mRNAs. Of these mRNAs, we observed a

207 significant overlap with 222 of 494 of DE mRNAs between P3 and P5 (OR=2.09, p=7.51e-15) and

208 1,091 of the 3,545 DE mRNAs between P5 and P7 (OR=1.18, p=3.79e-4).

209 Small RNA-seq analysis showed 153 DE miRNAs between sham and LAD three days post ligation,

210 followed by a marked decline in the number of DE miRNAs between sham and LAD at later time points

211 (Figure 4D). The top 40 significantly DE miRNAs between sham and LAD at P3 have not been

212 previously reported as DE following LAD ligation (Figure 4E). The 153 DE miRNAs identified

213 between sham and LAD at P3 are predicted to target 2,231 mRNAs. Of these 2,231 mRNAs, 1,090

214 overlap with the 2,741 DE mRNAs identified between sham and LAD at P3 (OR=2.06, p<2.2e-16).

215 Of the 39 DE miRNAs that correlated with and have predicted targets amongst the DE mRNAs, 14

216 miRNAs target gene sets of between 9 and 314 genes in pathways for cancer, and 14 miRNAs target

217 between 13 and 23 mRNAs in focal adhesion (Figure 4E, Data supplement 10). Interestingly, 31 of 39

218 miRNAs were conserved in humans and targeted a median of 75.7% of the orthologous genes in

219 corresponding human pathways. Mirroring the mRNA data, 83% of the miRNAs that were DE between

220 sham and LAD were also DE in the pairwise comparisons between the physiological time points (Figure

221 4F).

222 Functional analysis of miR inhibition and overexpression in P5 mouse cardiomyocytes

223 To test the functional effects of miRNAs on cardiomyocyte proliferation we performed inhibition and

224 overexpression studies in mouse and human cardiomyocytes, on a set of miRNAs that exhibited

225 significant changes in physiological and pathological conditions and correlated with changes in mRNA

226 in focal adhesion pathway We obtained over 80% reduction of the expression of nine miRNAs in

227 primary mouse cardiomyocytes and a subset of four of their human orthologues in iCell®

228 cardiomyocytes, and over 50% overexpression of miR-6240 (data not shown). qRT-PCR analysis of

229   the expression of cell cycle-regulating cyclins revealed that the levels of *Ccna2*, *CcnD2* and *CcnE2*

230   increased significantly (> 2-fold) following treatment with miR-22-5p, miR-451a and miR-195a

231   inhibitors, and with miR-6240 mimic, in comparison to cells treated with scramble ($p < 0.05$) (Figure

232   5A). Treatment with seven other miR inhibitors did not result in any significant changes ($p > 0.05$) of

233   tested cyclins expression (Figure 5A). Expression of *Ccna1*, *CcnD1*, *CcnD3* and *CcnE1* did not change

234   in response to inhibition or overexpression of any of the miRNAs.

235   To determine whether inhibition or overexpression of these miRs plays a direct role in promoting

236   cardiomyocyte proliferation we measured the nuclear incorporation of EdU (S-phase marker) and pH3

237   staining (mitosis marker) in P5 mouse cardiomyocytes. A marked increase in proliferating (EdU

238   positive) cells (up to 5-fold) was observed for cardiomyocytes treated with miR-22-5p, miR-144-3p,

239   miR-148a-3p, miR-193a-3p, miR-193b-3p, miR-195a-5p, miR-221-3p, miR-331-3p, miR-451a

240   inhibitors and miR-6240 mimic (Figure 5B). Likewise, an increase of mitotic (pH3 positive) cells was

241   seen (up to 3-fold), following treatment with miR-22-5p, miR-195a-5p and miR-451a inhibitors and

242   miR-6240 mimic (Figure 5C, Data supplement 11A). Scramble-treated mouse cells served as the

243   negative control for both assays.

244   **Functional analysis of selected miRs in human cardiomyocytes**

245   Given our data showing that several miRNAs regulate aspects of proliferation in P5 mouse

246   cardiomyocytes, we tested whether the human orthologues of these miRNAs can functionally regulate

247   cardiomyocyte proliferation in iCell® cardiomyocytes. We transfected iCell® cardiomyocytes with a

248   subset of human miR inhibitor and mimic orthologues that we had previously tested in mouse

249   cardiomyocytes. qRT-PCR analysis of cyclins expression revealed elevated levels of *Ccna2*, *CcnD2*

250   and *CcnE2* in miR-22-5p, miR-451a and miR-6240 treated cells in comparison with scramble treatment

251   ($p < 0.05$) (Figure 5D). As with the mouse miR interventions, levels of *Ccna1*, *CcnD1*, *CcnD3* and

252   *CcnE1* were unchanged (Figure 5D). iCell® cardiomyocytes treatment with miR-6240 mimic showed

253   an increase in number of proliferating cells and treatment with miR-144-3p, miR-195a-5p, miR-451a

254 and miR-6240 showed up to a 2–fold increase in the number of mitotic cells (Figure 5E, F, Data

255 supplement 11B).

Discussion

257 We set out to define the programme of the coding and non-coding transcriptome in the healthy neonatal

258 heart during the period of loss of regenerative capacity and to relate this to the transcriptional changes

259 associated with cardiac regeneration following neonatal MI. We found a sharp transition in microRNA

260 expression in the developing heart between P3 and P5 associated with subsequent changes in expression

261 of genes on the focal adhesion pathway and cardiomyocyte division arrest. We mapped profound

262 changes in the transcriptome that returned to normal within 10 days following neonatal MI, indicating

263 essentially complete healing of the myocardium by this time point, confirming our previous findings

264 [15]. We showed that two thirds of all RNA species that were DE in the post-MI heart were also DE

265 during normal postnatal development, suggesting a common regulatory pathway for normal post-natal

266 cardiac development and post-MI regeneration. Finally, we demonstrated that miR-144-3p, miR-195a-

267 5p and miR-451a inhibition and miR-6240 activation have functionally conserved roles in cell

268 proliferation and mitosis in mouse and human cardiomyocytes.

269 We found that the first 10 days of postnatal life were associated with alterations in gene expression of

270 thousands of genes, particularly those encoding proteins involved in cell cycle progression at early time

271 points, oxidative phosphorylation at later time points and protein translation throughout. These enriched

272 pathways are likely reflective of changes in ventricular pressure, transition from hypoxic to the oxygen

273 rich postnatal environment with increased reliance on oxidative metabolism, and changes in cellular

274 architecture and the extracellular matrix between P3 and P7 [13, 29]. During the P5 and P7 time

275 window, one quarter of the most DEG correspond to GO terms associated with M-phase mitosis and

276 mitotic cell cycle checkpoint, including *Cdk1* [30], *Ccna2* [31], *Cdc13* [32] and *Bub1* [33], in keeping

277 with the withdrawal of cardiomyocytes from DNA replication and cell division at this time point. While

278 the relative abundance of myocytes, cardiac fibroblasts, endothelial cells and vascular smooth muscle

279 cells change in the LV during the first ten postnatal days [34] and ontologies and pathways identified

280 through our transcriptomic study are in part reflective of this, we were able to identify putative drivers

281 of cardiomyocyte proliferation and functionally validate them in mouse primary cells and human

282 cardiomyocyte cell line.

283 We found major differences in mRNA, miRNA and lncRNA expression between LAD-ligated and

284 sham-operated mice three days following MI, but these differences had almost completely resolved

285 within seven days of LAD ligation and increased gene expression of cardiomyocyte markers is restored

286 to mirror closely the physiological gene expression changes. At the transcriptional level, therefore, the

287 regenerative process was essentially complete by P10, although certain developmental and cardiac

288 failure markers, like *Nppa* [35], remained elevated. The most profoundly DEG three days post LAD

289 were those involved in immune processes, similarly shown in the contrasting model of heart

290 regeneration following apex removal together with cell cycle progression and RNA synthesis [27] and

291 oxidative phosphorylation, in keeping with previous observations of the importance of an active

292 immune response in physiological regulation of cardiac regeneration in mice [36, 37].

293 Similar changes in expression were observed with lncRNAs, where of the 107 DE lncRNAs between

294 P5 and P7, only seven, including *H19* and *Neat1*, have proposed functions, in cell proliferation [38-40],

295 and none have been previously associated with postnatal heart development or regeneration. We also

296 found evidence for *trans*-regulation of expression by lncRNAs with enrichment amongst correlating

297 gene sets on OXPHOS, ribosomes and focal adhesion pathways, and show significant enrichment for

298 imprinting amongst DE lncRNAs. While previously described in other tissues [41], enrichment for

299 imprinted loci has rarely been observed previously in the postnatal heart or following MI [42].

300 We observed a profound shift in microRNA expression in the developing heart between P3 and P5

301 associated with an altered expression of genes on the focal adhesion pathway between P5 and P7. Since

302 genes and proteins on the focal adhesion pathway mediate the transduction of external stimuli such as

303 increasing blood pressure or hypoxia [29, 43, 44] into processes such as DNA replication and cell

304 division [45], we hypothesise that the set of miRNAs that were DE in the P3 to P5 time window are key

305 to the regulation of molecular events leading to withdrawal of the cardiomyocyte from cell division in

306   the first week of life. To test this hypothesis, we performed *in vitro* inhibition and over-expression

307   studies on 10 miRNAs which exhibited significant changes in physiological and pathological

308   conditions. They include two miRNAs (miR-195a-5p and miR-22-5p) for which previous evidence has

309   been presented [20, 46]. Our results demonstrate that the inhibition of miR-22-5p and miR-451a and

310   miR-6240 up-regulation individually elevate the expression of *CcnA2*, *CcnD2* and *CcnE2* in P5 mouse

311   and human cardiomyocytes leading to increased proliferation and cell division. We did not observe

312   changes in expression of *CcnA1* (expressed in germ cells), *CcnE1* (lowly expressed in heart), *CcnD1* or

313   *CcnD3* (low expression in tested cardiomyocytes) in comparison to scramble-treated cells. Targets of

314   miR-22 include *Map2k1*, *Map3k9*, *Rock2* representing the focal adhesion pathway, regulation of cell

315   proliferation, and *Aurkb* participating in the regulation of alignment and segregation of chromosomes

316   during cell division [47]. miR-451a targets *Tbx1* and *Ybx1* transcription factors regulating proliferation

317   and differentiation of multipotent heart progenitors [48] and is implicated in translational control of

318   foetal myocardial gene expression after cardiac transplant [49]. There is limited knowledge on the

319   functional role of miR-6240, and here we show for the first time, its function in cardiomyocyte

320   proliferation and heart regeneration in mouse and human cardiomyocytes [50]. Interestingly, miR-22

321   has been previously found to be highly expressed in cardiac muscle, upregulated during myocyte

322   differentiation which alone has been found to be sufficient to induce cardiomyocyte hypertrophy.

323   Our study reports the transcriptional changes in the developing and post-MI postnatal heart and defines

324   sets of mRNAs, miRNAs and lncRNAs that we propose to be the key regulators, at the level of the

325   transcriptome, of withdrawal of the postnatal mouse heart from DNA replication and cell division. We

326   also identify miR-144-3p, miR-195a, miR-451a and miR-6240 as functionally conserved, non-coding

327   regulators of cardiomyocyte division in neonatal mouse and humans. Whilst we have not studied all the

328   downstream consequences of our findings, including more detailed impact on protein, cell cycle, and

329   *in vivo* validation, our work provides a platform for future studies.

330   Recent progress in research in developmental cardiology has significantly advanced our understanding

331   of heart development and regeneration [51]. Insights from zebrafish models of heart regeneration,

332   following apex removal or cryosurgery, show that they are capable of myocardial regeneration mediated

333   mainly through the proliferation of pre-existing gata4$^+$ cardiomyocytes with miR-133 [52] and miR-

334   101 [53], playing regulatory roles in this process, as also shown in our neonatal mouse data set. More

335   recently, the attempt to pinpoint the regulatory hubs in zebrafish heart regeneration revealed a function

336   of i*l6st*, *adam8*, and *cd63* [19], also shown to be DE expressed in our post-ligation data sets. Studies of

337   heart regeneration in neonatal mice reported *Myh7* and *Igf1r* as key drivers of gene interaction networks

338   and pointing to *C1orf61*, *Aif1*, *Rock1* as potential inhibitors of cardiomyocyte proliferation and G1/S

339   phase transition [54], genes that were also DE between physiological time points in our set. In addition,

340   miRNAs from the miR-15 family [20], miR-503-5p [54], miR-199a [55], miR-99/100 and Let7a/c [21]

341   were also reported as critical regulators of the regeneration process, which were also found as DE in

342   our physiological and sham/LAD comparisions in our data set. Interleukin 13, DE in the regenerating

343   neonatal heart in our data set, has also been identified as a regulator of cardiomyocyte cell cycle entry

344   mediated by STAT3/periostin and STAT6 [27]. Whilst our data show considerable overlap with

345   previous observations in mice and zebrafish, we provide a systematic and comprehensive analysis of

346   coding and non-coding transcriptome changes over multiple time points of the first 10 days of postnatal

347   life and after neonatal LAD ligation, which has not been available hitherto.

348   In summary, we present a finely grained time course for mRNA, miRNA and lncRNA in the normal

349   developing heart from postnatal day 1 (P1) to P10, and in the 3 to 10 days following neonatal MI. We

350   found profound changes in the coding and non-coding transcriptome after neonatal MI, with evidence

351   of essentially complete transcriptional healing by P10. We find a sharp transition in miRNA expression

352   in physiological cardiac samples between P3 and P5, with differentially expressed miRNAs associated

353   specifically with altered expression of genes on the focal adhesion pathway and cessation of

354   cardiomyocyte division. Two thirds of each of the mRNAs, lncRNAs and microRNAs that were

355   differentially expressed in the post-MI heart were also differentially expressed during normal postnatal

356   development, suggesting a common regulatory pathway for normal cardiac development and post-MI

357   cardiac regeneration. Of the miRNAs that we implicate in regulation of cardiomyocyte development

358   and regeneration, 67% had targets that were conserved between mice and humans. We present a subset

359 of miRNAs: miR-451a, miR-6240, miR-195a-5p and miR-144-3p that showed functional evidence *in*

360 *vitro* as regulators of cell division in mouse and/or human cardiomyocytes.

Acknowledgements

Sources of Funding

Disclosures

372 None

Accession Number

374 Reads are deposited in ArrayExpress under accession code E-MTAB-3171.

375

Figure legends
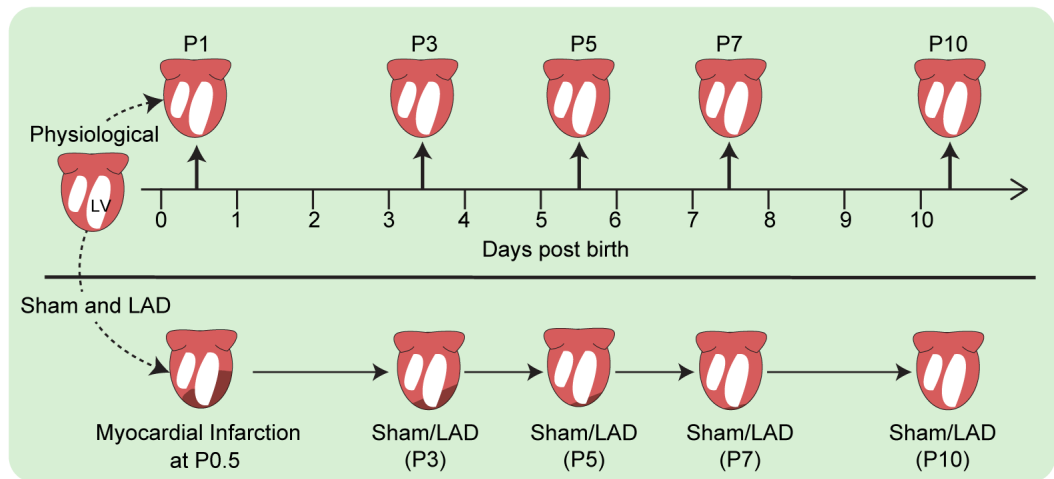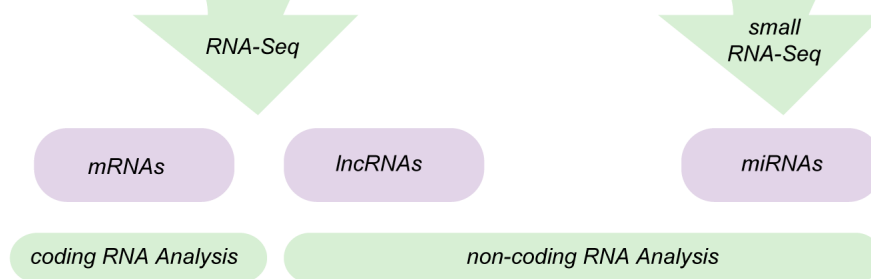
Figure1. Experimental design.

378 Overview of experimental design showing time points at which LV tissue was harvested (A) during

379 physiological time points, and following LAD or sham operation. P1-10, postnatal days 1-10; MI

380 myocardial infarction, (B) sequencing pipeline and (C) functional investigation.

A   Harvested LV from mouse heart

B   Sequencing & Analysis

C   Functional Investigation
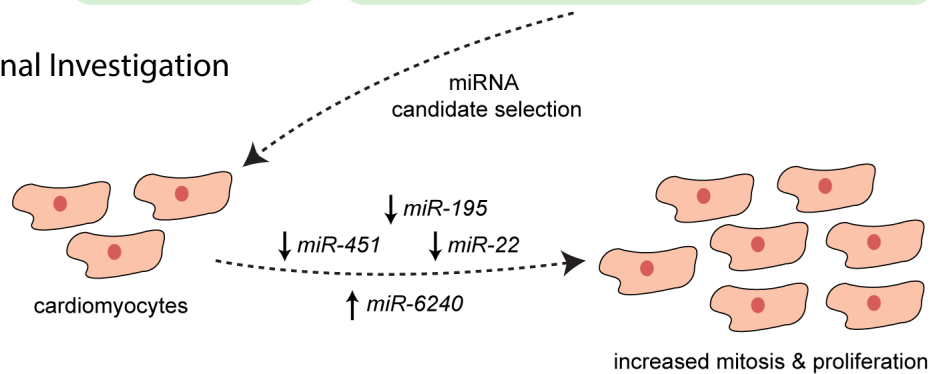
381

382

383 **Figure 2.** Changes of mRNA expression in physiological LV and following MI.

384 (A)   KEGG pathway analysis between adjacent pairwise comparisons in physiological LV. (B)

385 Venn diagram showing numbers of DE mRNAs between physiological pairwise comparison (C) Top

386 40 DE mRNAs between P5 and P7, (D) DE expressed transcripts between LAD and Sham samples-

387 pairwise comparison, (E) KEGG pathway analysis between LAD and Sham samples is pairwise

388 comparison, (F) Top 40 DE mRNAs between LAD and Sham 3 days post-surgery, (G) Overlap between

389 DE coding transcripts in physiological and MI LVs.
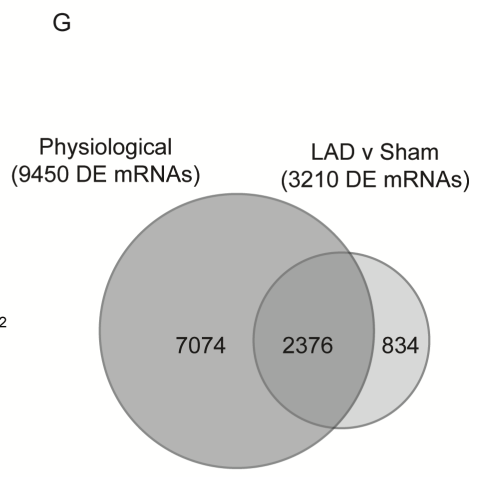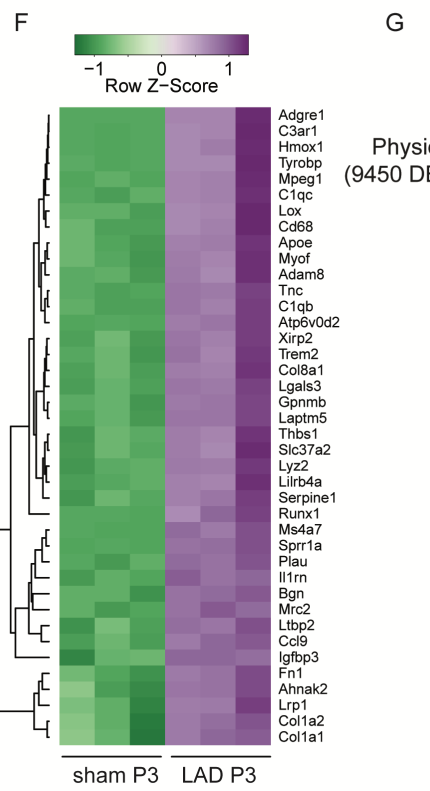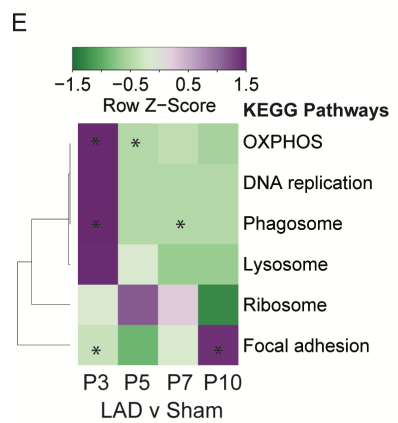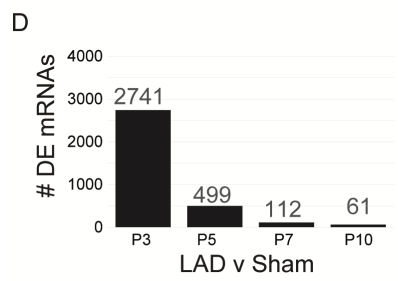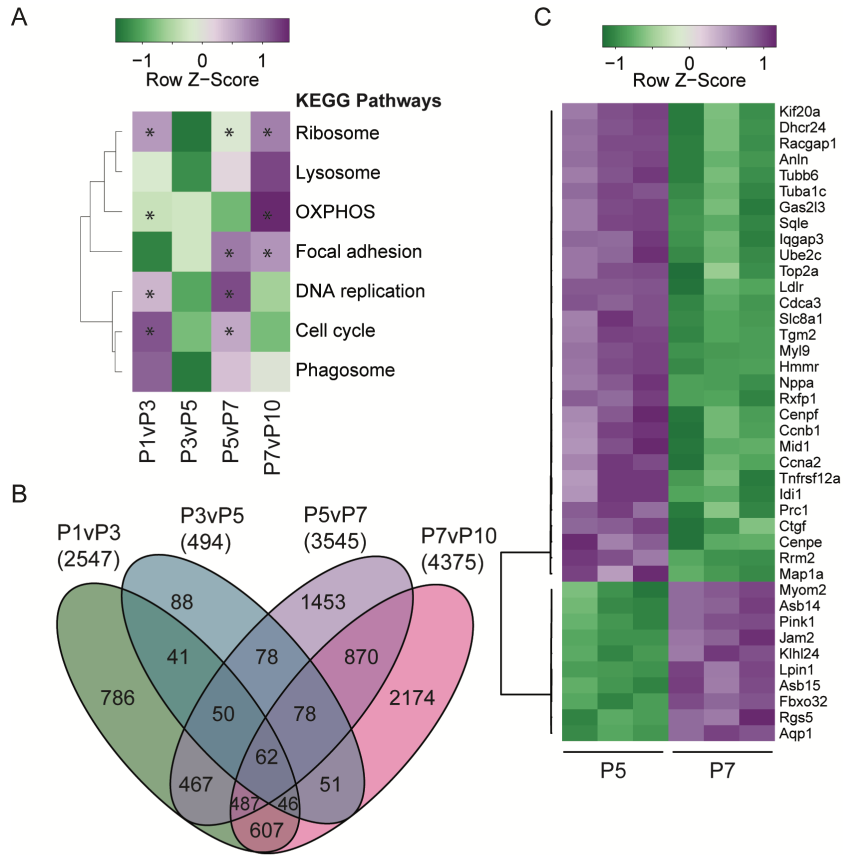
392　**Figure 3.** Changes of lncRNA expression in physiological LV and following MI.

393　(A) Venn diagram showing numbers of DE lncRNAs between adjacent pairwise comparisons in

394　physiological time points. (B) Top 40 most DE transcripts between P5 and P7. (C) The number of

395　correlating DE mRNAs with DE lncRNAs in the increasing distance from transcription start site (TSS).

396　(D) Numbers of DE lncRNAs following Sham and LAD operations in pairwise comparisons. (E)

397　Identities of the most DE lncRNAs between Sham and LAD-operated LVs three days post-surgery. (F)

398　Overlap between DE lncRNAs between physiological LVs and following surgery.
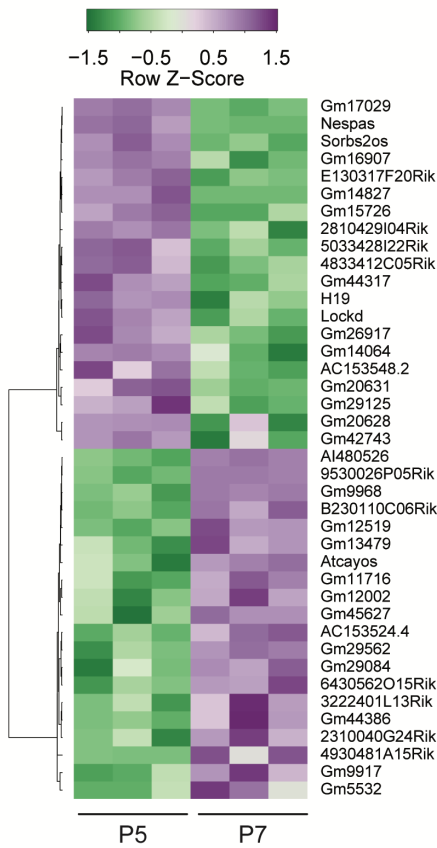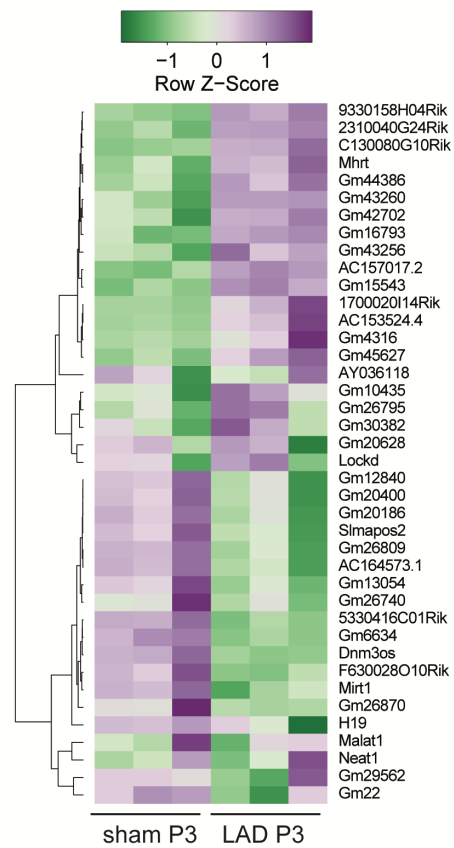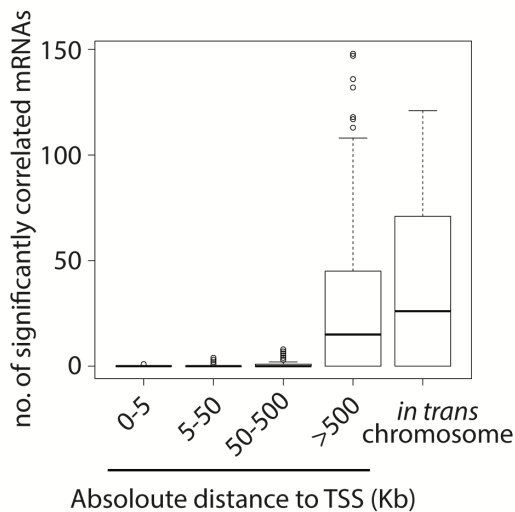
A

B

C

D

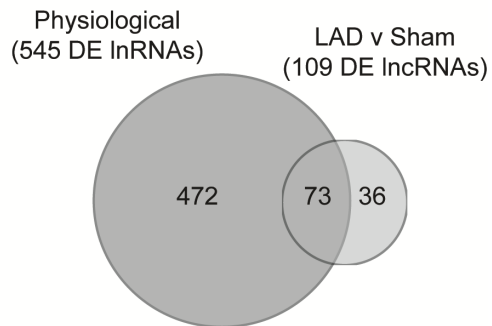
E
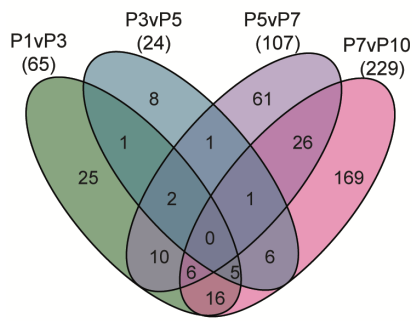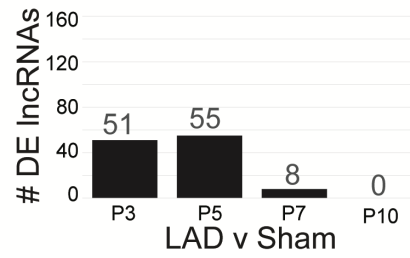
F

400   **Figure 4.** Changes of miRNA expression in physiological LV and following MI.

401   (A) Venn diagram showing numbers of DE miRNAs between adjacent pairwise comparisons in

402   physiological time points. (B) Heat map showing 40 most DE expressed miRNAs. (C) Focal adhesion

403   and growth factor pathways diagram showing the genes targeted by DE miRNAs. (D) Numbers of DE

404   miRNAs following MI. (E) Heat map of the most DE miRNAs three days post MI. (F) Overlap between

405   DE miRNAs between physiological LVs and following surgery.
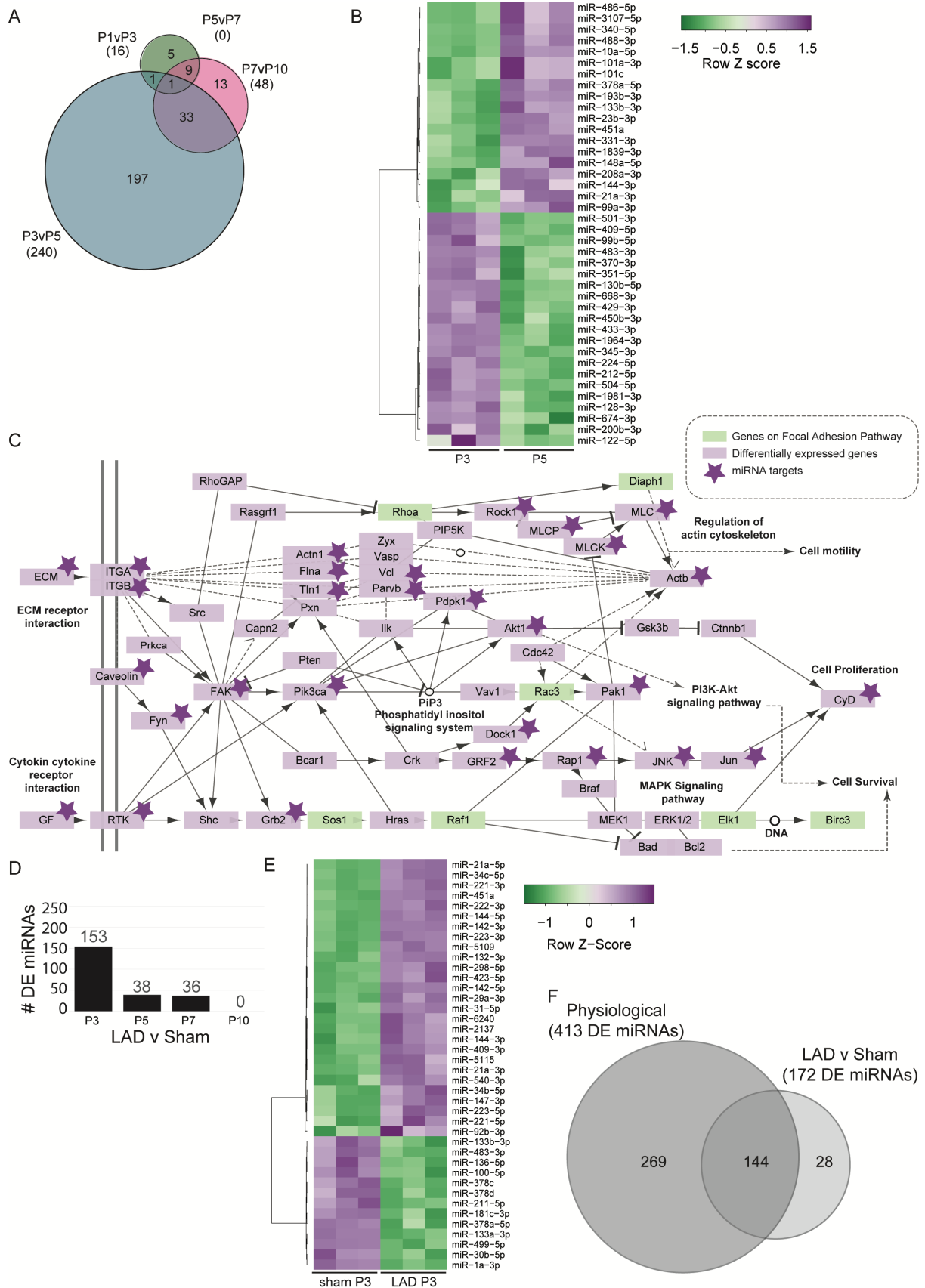
Figure 5. Functional analysis of miR inhibition and overexpression in P5 mouse and human cardiomyocytes.

(A) Changes in mRNA expression of cell cycle regulating cyclins in P5 mouse primary cardiomyocytes following treatment with miRNA inhibitors and mimic. A significance indicated by star. EdU and pH3 staining revealing number of proliferating (B) and dividing cells (C) following treatment with miRNAs. (D) Changes in mRNA expression of cell cycle regulating cyclins in human iPSC derived cardiomyocytes following treatment with miRNA inhibitors and mimic. A significance indicated by star. EdU and pH3 staining revealing number of proliferating (E) and dividing cells (F) iPSC derived cardiomyocytes following treatment with miRNAs. *** $p \leq 0.001$, ** $p \leq 0.01$, * $p \leq 0.05$.

A Neonatal mouse

D Human iPSC

B EdU

C pH3

E EdU

F pH3

References
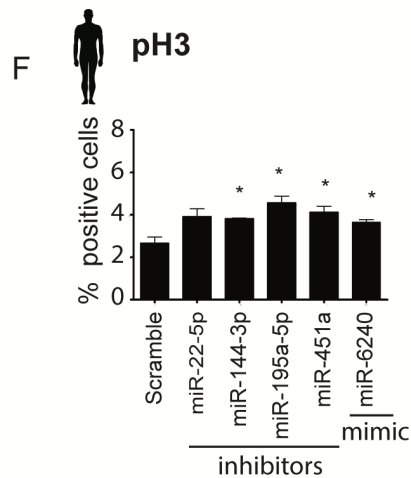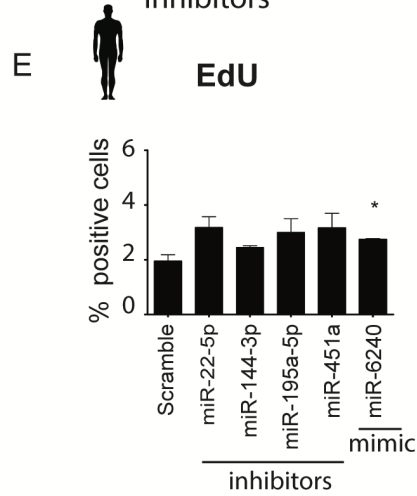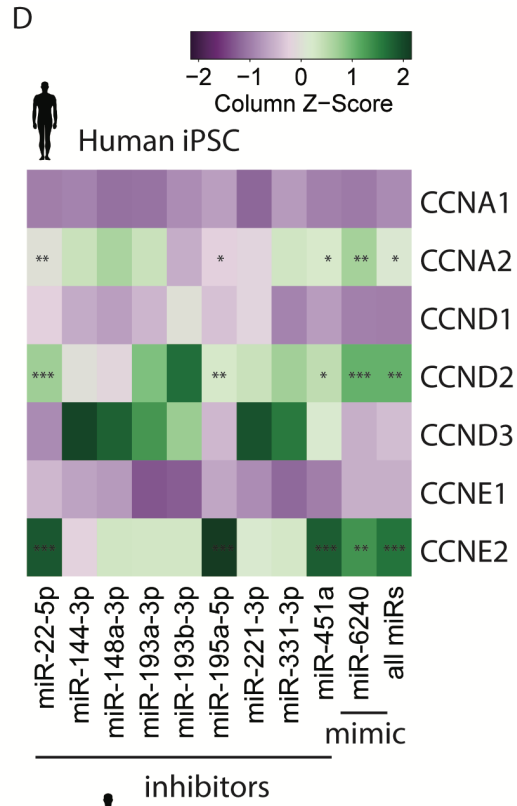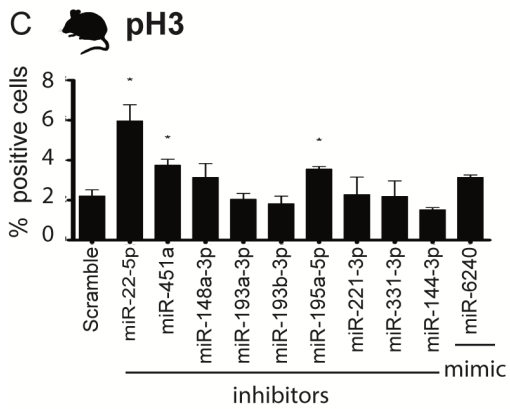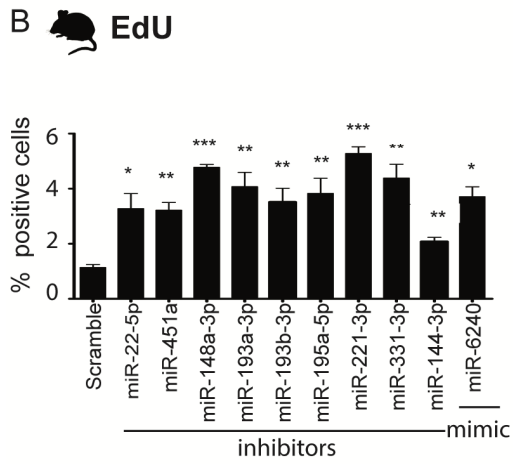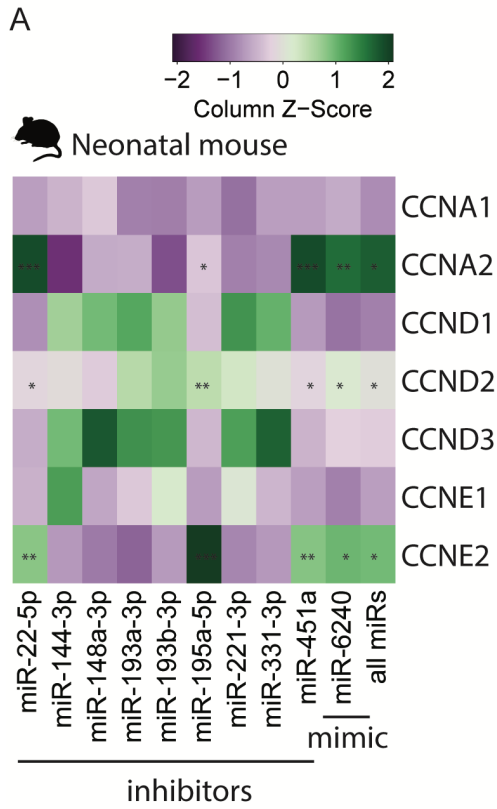
1. Moran AE, Forouzanfar MH, Roth GA, Mensah GA, Ezzati M, Murray CJ, Naghavi M: **Temporal trends in ischemic heart disease mortality in 21 world regions, 1980 to 2010: the Global Burden of Disease 2010 study.** *Circulation* 2014, **129:**1483-1492.

2. Schnapp E, Kragl M, Rubin L, Tanaka EM: **Hedgehog signaling controls dorsoventral patterning, blastema cell proliferation and cartilage induction during axolotl tail regeneration.** *Development* 2005, **132:**3243-3253.

3. Nacu E, Tanaka EM: **Limb regeneration: a new development?** *Annu Rev Cell Dev Biol* 2011, **27:**409-440.

4. Mahmoud AI, O'Meara CC, Gemberling M, Zhao L, Bryant DM, Zheng R, Gannon JB, Cai L, Choi WY, Egnaczyk GF, et al: **Nerves Regulate Cardiomyocyte Proliferation and Heart Regeneration.** *Dev Cell* 2015, **34:**387-399.

5. Wagers AJ, Conboy IM: **Cellular and molecular signatures of muscle regeneration: current concepts and controversies in adult myogenesis.** *Cell* 2005, **122:**659-667.

6. Seifert AW, Kiama SG, Seifert MG, Goheen JR, Palmer TM, Maden M: **Skin shedding and tissue regeneration in African spiny mice (Acomys).** *Nature* 2012, **489:**561-565.

7. Jugdutt BI, Joljart MJ, Khan MI: **Rate of collagen deposition during healing and ventricular remodeling after myocardial infarction in rat and dog models.** *Circulation* 1996, **94:**94-101.

8. Lutgens E, Daemen MJ, de Muinck ED, Debets J, Leenders P, Smits JF: **Chronic myocardial infarction in the mouse: cardiac structural and functional changes.** *Cardiovasc Res* 1999, **41:**586-593.

9. Naqvi N, Li M, Calvert JW, Tejada T, Lambert JP, Wu J, Kesteven SH, Holman SR, Matsuda T, Lovelock JD, et al: **A proliferative burst during preadolescence establishes the final cardiomyocyte number.** *Cell* 2014, **157:**795-807.

10. Alkass K, Panula J, Westman M, Wu TD, Guerquin-Kern JL, Bergmann O: **No Evidence for Cardiomyocyte Number Expansion in Preadolescent Mice.** *Cell* 2015, **163:**1026-1036.

11. Li F, Wang X, Capasso JM, Gerdes AM: **Rapid transition of cardiac myocytes from hyperplasia to hypertrophy during postnatal development.** *J Mol Cell Cardiol* 1996, **28:**1737-1746.

12. Soonpaa MH, Kim KK, Pajak L, Franklin M, Field LJ: **Cardiomyocyte DNA synthesis and binucleation during murine development.** *Am J Physiol* 1996, **271:**H2183-2189.

13. Puente BN, Kimura W, Muralidhar SA, Moon J, Amatruda JF, Phelps KL, Grinsfelder D, Rothermel BA, Chen R, Garcia JA, et al: **The oxygen-rich postnatal environment induces cardiomyocyte cell-cycle arrest through DNA damage response.** *Cell* 2014, **157:**565-579.

14. Porrello ER, Mahmoud AI, Simpson E, Hill JA, Richardson JA, Olson EN, Sadek HA: **Transient regenerative potential of the neonatal mouse heart.** *Science* 2011, **331:**1078-1080.

15. Haubner BJ, Adamowicz-Brice M, Khadayate S, Tiefenthaler V, Metzler B, Aitman T, Penninger JM: **Complete cardiac regeneration in a mouse model of myocardial infarction.** *Aging (Albany NY)* 2012, **4:**966-977.

16. Porrello ER, Mahmoud AI, Simpson E, Johnson BA, Grinsfelder D, Canseco D, Mammen PP, Rothermel BA, Olson EN, Sadek HA: **Regulation of neonatal and adult mammalian heart regeneration by the miR-15 family.** *Proc Natl Acad Sci U S A* 2013, **110:**187-192.

17. Tanaka EM, Reddien PW: **The cellular basis for animal regeneration.** *Dev Cell* 2011, **21:**172-185.

18. Sikes JM, Newmark PA: **Restoration of anterior regeneration in a planarian with limited regenerative ability.** *Nature* 2013, **500:**77-80.

19. Rodius S, Androsova G, Gotz L, Liechti R, Crespo I, Merz S, Nazarov PV, de Klein N, Jeanty C, Gonzalez-Rosa JM, et al: **Analysis of the dynamic co-expression network of heart regeneration in the zebrafish.** *Sci Rep* 2016, **6:**26822.

466 20. Porrello ER, Johnson BA, Aurora AB, Simpson E, Nam YJ, Matkovich SJ, Dorn GW, 2nd, van
467   Rooij E, Olson EN: **MiR-15 family regulates postnatal mitotic arrest of cardiomyocytes.** *Circ*
468   *Res* 2011, **109:**670-679.
469 21. Aguirre A, Montserrat N, Zacchigna S, Nivet E, Hishida T, Krause MN, Kurian L, Ocampo A,
470   Vazquez-Ferrer E, Rodriguez-Esteban C, et al: **In vivo activation of a conserved microRNA**
471   **program induces mammalian heart regeneration.** *Cell Stem Cell* 2014, **15:**589-604.
472 22. Grote P, Wittler L, Hendrix D, Koch F, Wahrisch S, Beisaw A, Macura K, Blass G, Kellis M, Werber
473   M, Herrmann BG: **The tissue-specific lncRNA Fendrr is an essential regulator of heart and**
474   **body wall development in the mouse.** *Dev Cell* 2013, **24:**206-214.
475 23. Klattenhoff CA, Scheuermann JC, Surface LE, Bradley RK, Fields PA, Steinhauser ML, Ding H,
476   Butty VL, Torrey L, Haas S, et al: **Braveheart, a long noncoding RNA required for**
477   **cardiovascular lineage commitment.** *Cell* 2013, **152:**570-583.
478 24. Han P, Li W, Lin CH, Yang J, Shang C, Nurnberg ST, Jin KK, Xu W, Lin CY, Lin CJ, et al: **A long**
479   **noncoding RNA protects the heart from pathological hypertrophy.** *Nature* 2014, **514:**102-
480   106.
481 25. Wang K, Liu CY, Zhou LY, Wang JX, Wang M, Zhao B, Zhao WK, Xu SJ, Fan LH, Zhang XJ, et al:
482   **APF lncRNA regulates autophagy and myocardial infarction by targeting miR-188-3p.** *Nat*
483   *Commun* 2015, **6:**6779.
484 26. Viereck J, Kumarswamy R, Foinquinos A, Xiao K, Avramopoulos P, Kunz M, Dittrich M, Maetzig
485   T, Zimmer K, Remke J, et al: **Long noncoding RNA Chast promotes cardiac remodeling.** *Sci*
486   *Transl Med* 2016, **8:**326ra322.
487 27. O'Meara CC, Wamstad JA, Gladstone RA, Fomovsky GM, Butty VL, Shrikumar A, Gannon JB,
488   Boyer LA, Lee RT: **Transcriptional reversion of cardiac myocyte fate during mammalian**
489   **cardiac regeneration.** *Circ Res* 2015, **116:**804-815.
490 28. Patro R, Duggal G, Love MI, Irizarry RA, Kingsford C: **Salmon provides fast and bias-aware**
491   **quantification of transcript expression.** *Nat Methods* 2017, **14:**417-419.
492 29. Goldmann WH: **Mechanotransduction and focal adhesions.** *Cell Biol Int* 2012, **36:**649-652.
493 30. Barr FA, Gruneberg U: **Cytokinesis: placing and making the final cut.** *Cell* 2007, **131:**847-860.
494 31. Kabeche L, Compton DA: **Cyclin A regulates kinetochore microtubules to promote faithful**
495   **chromosome segregation.** *Nature* 2013, **502:**110-113.
496 32. Pennock E, Buckley K, Lundblad V: **Cdc13 delivers separate complexes to the telomere for**
497   **end protection and replication.** *Cell* 2001, **104:**387-396.
498 33. Toledo CM, Herman JA, Olsen JB, Ding Y, Corrin P, Girard EJ, Olson JM, Emili A, DeLuca JG,
499   Paddison PJ: **BuGZ is required for Bub3 stability, Bub1 kinetochore function, and**
500   **chromosome alignment.** *Dev Cell* 2014, **28:**282-294.
501 34. Banerjee I, Fuseler JW, Price RL, Borg TK, Baudino TA: **Determination of cell types and**
502   **numbers during cardiac development in the neonatal and adult rat and mouse.** *Am J Physiol*
503   *Heart Circ Physiol* 2007, **293:**H1883-1891.
504 35. Matsuoka K, Asano Y, Higo S, Tsukamoto O, Yan Y, Yamazaki S, Matsuzaki T, Kioka H, Kato H,
505   Uno Y, et al: **Noninvasive and quantitative live imaging reveals a potential stress-responsive**
506   **enhancer in the failing heart.** *FASEB J* 2014, **28:**1870-1879.
507 36. Aurora AB, Porrello ER, Tan W, Mahmoud AI, Hill JA, Bassel-Duby R, Sadek HA, Olson EN:
508   **Macrophages are required for neonatal heart regeneration.** *J Clin Invest* 2014, **124:**1382-
509   1392.
510 37. Godwin JW, Pinto AR, Rosenthal NA: **Macrophages are required for adult salamander limb**
511   **regeneration.** *Proc Natl Acad Sci U S A* 2013, **110:**9415-9420.
512 38. Hao Y, Crenshaw T, Moulton T, Newcomb E, Tycko B: **Tumour-suppressor activity of H19 RNA.**
513   *Nature* 1993, **365:**764-767.
514 39. Keniry A, Oxley D, Monnier P, Kyba M, Dandolo L, Smits G, Reik W: **The H19 lincRNA is a**
515   **developmental reservoir of miR-675 that suppresses growth and Igf1r.** *Nat Cell Biol* 2012,
516   **14:**659-665.

517   40.   Yang F, Bi J, Xue X, Zheng L, Zhi K, Hua J, Fang G: **Up-regulated long non-coding RNA H19**
518   **contributes to proliferation of gastric cancer cells.** *FEBS J* 2012, **279:**3159-3165.
519   41.   Barlow DP, Bartolomei MS: **Genomic imprinting in mammals.** *Cold Spring Harb Perspect Biol*
520   2014, **6**.
521   42.   Menheniott TR, Woodfine K, Schulz R, Wood AJ, Monk D, Giraud AS, Baldwin HS, Moore GE,
522   Oakey RJ: **Genomic imprinting of Dopa decarboxylase in heart and reciprocal allelic**
523   **expression with neighboring Grb10.** *Mol Cell Biol* 2008, **28:**386-396.
524   43.   Balaban NQ, Schwarz US, Riveline D, Goichberg P, Tzur G, Sabanay I, Mahalu D, Safran S,
525   Bershadsky A, Addadi L, Geiger B: **Force and focal adhesion assembly: a close relationship**
526   **studied using elastic micropatterned substrates.** *Nat Cell Biol* 2001, **3:**466-472.
527   44.   Ross RS, Borg TK: **Integrins and the myocardium.** *Circ Res* 2001, **88:**1112-1119.
528   45.   Roovers K, Assoian RK: **Effects of rho kinase and actin stress fibers on sustained extracellular**
529   **signal-regulated kinase activity and activation of G(1) phase cyclin-dependent kinases.** *Mol*
530   *Cell Biol* 2003, **23:**4283-4294.
531   46.   Huang ZP, Wang DZ: **miR-22 in cardiac remodeling and disease.** *Trends Cardiovasc Med* 2014,
532   **24:**267-272.
533   47.   Nunes Bastos R, Gandhi SR, Baron RD, Gruneberg U, Nigg EA, Barr FA: **Aurora B suppresses**
534   **microtubule dynamics and limits central spindle size by locally activating KIF4A.** *J Cell Biol*
535   2013, **202:**605-621.
536   48.   Chen L, Fulcoli FG, Tang S, Baldini A: **Tbx1 regulates proliferation and differentiation of**
537   **multipotent heart progenitors.** *Circ Res* 2009, **105:**842-851.
538   49.   David JJ, Subramanian SV, Zhang A, Willis WL, Kelm RJ, Jr., Leier CV, Strauch AR: **Y-box binding**
539   **protein-1 implicated in translational control of fetal myocardial gene expression after**
540   **cardiac transplant.** *Exp Biol Med (Maywood)* 2012, **237:**593-607.
541   50.   Yang KC, Ku YC, Lovett M, Nerbonne JM: **Combined deep microRNA and mRNA sequencing**
542   **identifies protective transcriptomal signature of enhanced PI3Kalpha signaling in cardiac**
543   **hypertrophy.** *J Mol Cell Cardiol* 2012, **53:**101-112.
544   51.   Uosaki H, Cahan P, Lee DI, Wang S, Miyamoto M, Fernandez L, Kass DA, Kwon C:
545   **Transcriptional Landscape of Cardiomyocyte Maturation.** *Cell Rep* 2015, **13:**1705-1716.
546   52.   Yin VP, Lepilina A, Smith A, Poss KD: **Regulation of zebrafish heart regeneration by miR-133.**
547   *Dev Biol* 2012, **365:**319-327.
548   53.   Beauchemin M, Smith A, Yin VP: **Dynamic microRNA-101a and Fosab expression controls**
549   **zebrafish heart regeneration.** *Development* 2015, **142:**4026-4037.
550   54.   Gan J, Sonntag HJ, Tang MK, Cai D, Lee KK: **Integrative Analysis of the Developing Postnatal**
551   **Mouse Heart Transcriptome.** *PLoS One* 2015, **10:**e0133288.
552   55.   Eulalio A, Mano M, Dal Ferro M, Zentilin L, Sinagra G, Zacchigna S, Giacca M: **Functional**
553   **screening identifies miRNAs inducing cardiac regeneration.** *Nature* 2012, **492:**376-381.

554